# Preparation and multi-properties determination of radium-containing rocklike material

**Changshou Hong[1,2,3], Xiangyang Li[2], Guoyan Zhao[1], Fuliang Jiang[2], Ming Li[2], Shuai Zhang[2], Hong Wang[2] and Kaixuan Liu[2]**

[1] School of Resources and Safety Engineering, Central South University, Changsha, Hunan Province, 410083, China;
[2] School of Environmental and Safety Engineering, University of South China, Hengyang, Hunan Province, 421001, China.

[3] hongchangshou@163.com

**Abstract.** The radium-containing rocklike material were fabricated using distilled water, ordinary Portland cement and additives mixed aggregates and admixtures according to certain proportion. The physico-mechanical properties as well as radioactive properties of the prepared rocklike material were measured. Moreover, the properties of typical granite sample were also investigated. It is found on one hand, similarities exist in physical and mechanical properties between the rocklike material and the granite sample, this confirms the validity of the proposed method; on the other hand, the rocklike material generally performs more remarkable radioactive properties compared with the granite sample, while radon diffusive properties in both materials are essentially matching. This study will provide a novel way to prepare reliable radium-containing samples for radon study of underground uranium mine.

## 1. Introduction

Mining and milling activities involved natural uranium are the fundamental step in the front end of nuclear fuel cycle. It is well known that mineral extraction of uranium ores brings serious negative influence of exposure radiation to underground miners, such as lung cancer, its high incidence among the miners is proved closely related with excess inhalations of radon [1]. Thus rock-associated radon research for underground uranium mine, such as radon measurement and risk assessment, has attracted widespread attention [2]. Among the field of laboratory measurement of radon, the naturally obtained radioactive material, like stony material [3–5] or uranium ore rock [6–9] is widely used owing to its convenience, simplicity and the cost effectiveness. However, this kind of material itself as the sample for rigorous scientific research is not perfect yet, because there is no faithful method in guaranteeing the samples to be with consistent initial conditions. As to field measurement of radon in underground uranium mine, the large spatial scale and radiation hazards to the investigator will hinder long-term measurements [10].

In most cases, dealing with rock-associated engineering and scientific problems in the field of underground hard-rock mine are not simple tasks. Rock mechanics tests, for instance, are known as irreversibly destructive processes, yet field sampling hardly satisfies the extensive requirement for these tests. Fortunately, similarity theory provides a useful way to organize the variables involved in scientific or engineering issue to our maximum advantage, and guide the optimizing design of experiments to obtain the most information [11]. Especially, the Scale Model Test (SMT) method, based on similarity theory, is frequently utilized in laboratory to reconstruct various phenomena occurring in underground engineering, because the major factors in model test can be independently

controlled as needed. More importantly, this method is time- and labor-saving, and accessible to the preliminary optimization of testing protocol compared with field trials. Thus, the SMT method has been regarded as a reliable, applicable and promising method in the field of underground engineering [11–15]. Yet the utilization of SMT method for radon research associated with underground uranium mine has not been reported.

In this paper, aiming at meeting the heavy demand of samples or geo-mechanical models for radon research associated with underground uranium mine, radium-containing radioactive rocklike materials from the prototype of typical granite sample taken from South China were fabricated based on the principles of similarity theory. The physical, mechanical and radioactive properties of the prepared materials were investigated by comparing with the prototype sample.

## 2. Materials and methods

### *2.1. Raw materials and sample preparation*

*2.1.1. Raw materials* The ordinary Portland cement was used as the cementing agent (strength grade C42.5), the cement was overall control of the physical and mechanical properties of the rocklike material. In relation to the option of the remaining ingredients, any single ingredient only controls a certain property of the material, yet makes insignificant effect on its general properties. Therefore, on the basis of extensive references, pure quartz sands (silica purity>99.99%) mixed with uranium mill tailings ($^{226}$Ra content=$8.51\times10^{3}$ Bq kg$^{-1}$) were used as the aggregates, Table 1 displays the particle size distribution of the aggregates; silica fume (purity>99.99%) used for reducing the porosity of composite mortar and ferrous powder (purity>99.99%) for aggrandizing its volume weight were selected as the admixtures; early-strength agent and water-reducing agent (ratio=1:2) were used as the additives; besides, the used water were distilled.

**Table 1.** Particle size distribution of the aggregates.

| Particle size (mm) | Original tailings[a] (%) | Worked tailings[b] (%) | Quartz sands content[c] (%) |
|---|---|---|---|
| 2.36～4.75 | 0.08 | 7.58 | 99.32 |
| 1.18～2.36 | 0.93 | 12.25 | 95.06 |
| 0.60～1.18 | 7.66 | 21.01 | 76.40 |
| 0.30～0.60 | 57.62 | 37.32 | 0 |
| 0.15～0.30 | 16.33 | 10.58 | 0 |
| 0.075～0.15 | 12.27 | 7.95 | 0 |
| ＜0.075 | 5.11 | 3.31 | 0 |

[a] The part of tailings with the particle size larger than 4.75 mm was eliminated.
[b] The worked tailings refer to the tailings added with pure quartz sands.
[c] The quartz sands content means the proportion of quartz sands in the mixture within a certain particle size.

*2.1.2. Preparation processes* Considering the different characterizations of the above-mentioned ingredients, the preparation processes of the rocklike materials were divided into the following steps:

- The ingredients weighted by mass were in accordance with the proportion shown in Table 2.
- Mixing the granular ingredients like aggregates (pure quartz sands and uranium mill tailings), cementing agent (ordinary Portland cement) and admixtures (silica fume and ferrous powder) together in the concrete mixer, and stirring them well.
- Adding the distilled water to the dry mixture, and ensuring them to be well-stirring.
- Adding the additives (early-strength agent and water-reducing agent) into the wet mixture and guaranteeing thorough mixing.
- Scooping the well-stirred mixture carefully into the self-made moulds.
- To ensure higher compactness of the sample, putting the moulds containing the mixed ingredients on the vibration table, keeping them to be vibrated for 10–15 min.

- Demoulding and then curing the samples in appropriate temperature (20±1°C) and relative humidity (> 95%RH) for 28 days.
- Cutting the redundant rough ends of the samples utilizing Struers Secotom-15 cutting machine.

The specimens of the rocklike material, namely the moulded and cut samples, were shown in Figure 1.

**Table 2.** The proportions of the involved ingredients.

| Parameters | Cement | Silica fume | Ferrous powder |
|---|---|---|---|
| Mass portion | 1 | 0.12 | 0.25 |
| Proportion/% | 34.48 | 4.14 | 8.62 |
| Parameters | Additives | Aggregates | Distilled water |
| Mass portion | 0.03 | 1.2 | 0.3 |
| Proportion/% | 1.03 | 41.38 | 10.34 |

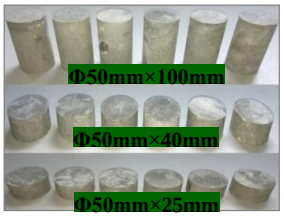


**Figure 1.** The rocklike materials.

*2.2. Properties determination*

*2.2.1. Physical parameters test* A total of 10 cylindrical specimens (diameter 50 mm, height 100 mm) were used to carry out the physical parameters test. In detail, the specimens were dried in an electric thermostatic drying oven (105±5 ℃, 48 h), after cooling them down, the mass of each specimen was then weighted by a precision balance (with accuracy of 0.01 g).

The dry density ($\rho_{dry}$, g cm$^{-3}$) of the rocklike material was determined by Eq. (1):

$$\rho_{dry} = M_{dry} / V \tag{1}$$

where $M_{dry}$ is the mass of specimen in dried state, g; $V$ is the volume of the specimen, cm$^{-3}$.

Grain density ($\rho_{grain}$, g cm$^{-3}$) of the rocklike material from 6 oven-dried granular samples (<5 mm) was determined using pycnometer method. The grain density $\rho_{grain}$ was determined by Eq. (2) [16]:

$$\rho_{grain} = \frac{M_{grain}\rho_{water}}{M_{water} + M_{grain} - M_{res\text{-}water}} \tag{2}$$

where $M_{grain}$ is the mass of particle sample in dried state, g; $M_{water}$ is the mass of water in pycnometer, g; $M_{res\text{-}water}$ is the total mass of residual water along with the sample in pycnometer, g; $\rho_{water}$ is the density of distilled water, namely 1.0 g cm$^{-3}$.

The porosity ($\eta$) of the rocklike material can be respectively estimated by Eq. (3) [17]:

$$\eta = \left[1 - \left(\rho_{dry} / \rho_{grain}\right)\right] \times 100\% \tag{3}$$

*2.2.2. Mechanical parameters test* Basic mechanical parameters of the rocklike material contains uniaxial compressive strength ($\sigma_c$, MPa), elastic modulus ($E$, MPa), Poisson ratio ($\mu$), tensile strength ($\sigma_t$, MPa), cohesion ($c$, MPa) and internal friction angle ($\varphi$, °).

(1) Tests of uniaxial compressive strength $\sigma_c$, elastic modulus $E$ and Poisson ratio $\mu$

Six cylindrical specimens (diameter 50 mm, height 100 mm were used in the tests, and the tests were carried out via TYE-600E compression testing machine (Wuxi Jianyi Instrument & Machinery Co., Ltd., China). In process of uniaxial compression, stress-strain curve of the specimen could be digitally displayed by the compression testing machine. The slope of stress-strain curve at elastic stage represents the elastic modulus of the rocklike material.

With regard to the test of Poisson ratio of the specimen, electrometric method by utilization of GM-1A-10 static resistance strain indicator (Qinhuangdao AFT Electronic Technology Co., Ltd., China) was employed. To be specific, strain gages were vertically and horizontally pasted on the surface of the specimen, and its axial and transversal deformations could be monitored via the strain indicator. Then, the Poisson ratio could be calculated by the following Eq. (4):

$$\mu = \varepsilon_x / \varepsilon_y \tag{4}$$

where $\varepsilon_x$ and $\varepsilon_y$ represents transversal and axial strains of the specimen, respectively.

(2) Brazilian test of tensile strength $\sigma_t$

Brazilian test was proved effective on the test of tensile strength [18,19]. Six cylindrical specimens (diameter 50 mm, height 25 mm) were used in the Brazilian test, and the TYE-600E compression testing machine was still employed. According to test results of pressure obtained by the compression testing machine, the tensile strength of the specimen can be determined by Eq. (5) [20]:

$$\sigma_t = \frac{2p}{\pi dh} \tag{5}$$

where $p$ is the peak load on the specimen when it is damaged, N; $d$ is the diameter of the specimen, namely 50 mm; $h$ is the height of the specimen, namely 25 mm; $\pi$ is circumference ratio.

(3) Tests of cohesion $c$ and internal friction angle $\varphi$

Six cylindrical specimens (diameter 50 mm, height 40 mm) were prepared for the tests of cohesion and internal friction angle. The YZ-30 direct shear apparatus (Jinan Haiweier Instrument Co., Ltd., China) was adopted in the tests. The shear strength of the specimen can be determined by Eq. (6) [21]:

$$\tau = \sigma \tan\varphi + c \tag{6}$$

where $\sigma$ is the normal stress, MPa; $\tau$ is the shear strength, MPa. The shear strength vs. normal stress curve of the specimens was shown in Figure 2.

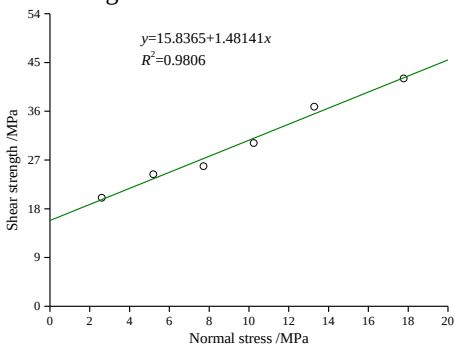


**Figure 2.** The shear strength vs. normal stress curve of the specimens.

*2.2.3. Radioactive parameters test* The concerned radioactive parameters contain surface radioactivity (i.e. dose equivalent rate) ($\dot{H}$, μSv $h^{-1}$), radium content ($C_{Ra}$, Bq $kg^{-1}$), radon exhalation rate ($J$, Bq $m^{-2}$ $s^{-1}$), radon diffusion coefficient ($D$, $m^2$ $s^{-1}$), radon diffusion length ($L$, m) and radon emanation fraction ($f$).

(1) Test of surface radioactivity $\dot{H}$

Nine cylindrical specimens (two thirds with 50 mm diameter and 25 mm height, the others with 50 mm diameter and 100 mm height) were used in the tests of surface radioactivity. One base of the specimen was exposed for radioactivity measurement, while the other surface of the specimen was sealed by aluminum foil (see Figure 3). The detector was RM250 gamma meter, produced by Shanghai Chaoqi Electronic Co., Ltd., China. Before carrying out the tests, background radioactivity where the tests were carried out has been checked.

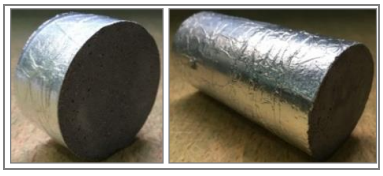

**Figure 3.** The specimens partially sealed by aluminum foil.

(2) Determination of radium content $C_{Ra}$

The six known quantities (0.5012 g, 0.5017 g, 0.5020 g, 0.5022 g, 0.5031 g and 0.5038 g) of oven-dried powder samples in the size smaller than 0.074 mm were used for the measurement of radium

content, and the scintillation chamber method was adopted in this study [22]. Each sample was repeatedly leached by using aqua regia, and the microwave digestion instrument (Milestone International Co., Ltd., Italy) was used for the digestion of the solution. After that and till the solution cooled down, it was transferred to a bubbler connected to a scintillation chamber for radon accumulation and collection. Subsequently, the FD-125 radon and thorium analyser (CNNC Beijing Nuclear Instrument Factory, China) along with the GW1016 scaler (Beijing Explore Times Technology Co., Ltd., China) were adopted to read the data of radon activity concentrations. Eq. (7) shows the calculation formula for obtaining radium content.

$$C_{\mathrm{Ra}} = \frac{k_{\mathrm{s}} V_{\mathrm{s}} (n - n_0)}{m \cdot (1 - \mathrm{e}^{-\lambda T})} \tag{7}$$

where $k_s$ is the calibration factor of scintillation chamber, Bq m$^{-3}$ cpm$^{-1}$; $V_s$ is the volume of scintillation chamber, m$^3$; $m$ is the weight of the powder sample, kg; $\lambda$ is the decay constant of radon, $\lambda = 2.1 \times 10^{-6}$ s$^{-1}$; $T$ is the build-up time in the bubbler, s; $n_0$ is the background counting rate of the scintillation chamber, cpm; $n$ is the total counting rate (including the background portion and sample portion) of the scintillation chamber, cpm.

(3) Determinations of radon exhalation rate $J$ and radon diffusive parameters ($D$ and $L$)

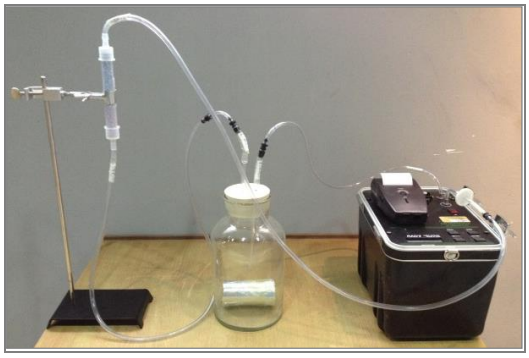

**Figure 4.** Apparatus for the measurement of radon exhalation rate.

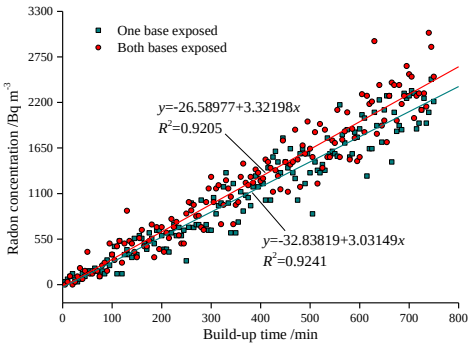


**Figure 5.** Measured radon concentrations along with the fitted trend lines.

The closed chamber radon-flux method [23,24] was adopted to test radon exhalation rate and radon diffusion coefficient in the rocklike material. Figure 4 presents the experimental setup consisting of several components: RAD7 radon monitors (DURRIAGE Corp., U.S.), iron support, desiccant (W.A. Hammond Drierite Co., Ltd., U.S.), accumulation jar with rubber lid, glass tubes, vinyl pipes, filter sieve and the specimens. The specimen (diameter 50 mm, height 100 mm) partially sealed by aluminum foil (two cases: one exposed base and two exposed bases) was used in the tests. Specially, the elimination of background radioactivity before each test was of necessity. In detail, anhydrous alcohol was used to clean the accumulation jar and the rubber lid, and let them be naturally dried in dry and ventilated place. The following step was assembling the setup and purging the system for 15–20 min, and following with the measurement of background radon concentration of the accumulation jar. Repeat the purge step if the measured radon concentration was higher than the laboratory background level. Thereafter, we carried out the continuous measurements (five minutes for an interval, within a total build-up time of 12.5 h) of radon accumulative concentrations (see Figure 5).

From the Figure 5, surface radon exhalation rates under the situation with one or two exposed bases, respectively denoted as $J_1$ (Bq m$^{-2}$ s$^{-1}$) and $J_2$ (Bq m$^{-2}$ s$^{-1}$), can be obtained by Eqs. (8) and (9):

$$J_1 = \frac{V_{\mathrm{acum}} \cdot \Delta C_{\mathrm{Rn}}}{S_{\mathrm{exposed},1} \cdot \Delta T} = \frac{k_1 V_{\mathrm{acum}}}{6000 S} \tag{8}$$

$$J_2 = \frac{V_{\mathrm{acum}} \cdot \Delta C_{\mathrm{Rn}}}{S_{\mathrm{exposed},2} \cdot \Delta T} = \frac{k_2 V_{\mathrm{acum}}}{12000 S} \tag{9}$$

where $V_{acum}$ is the accumulative volume of radon in the accumulation jar, $cm^3$; $S$ is the cross-sectional area of the specimen, $S = 19.63\ cm^2$; $S_{exposed,1}$ and $S_{exposed,2}$ are the exposed surface areas of the specimens respectively under above-mentioned conditions, namely $S_{exposed,1} = S$ and $S_{exposed,2} = 2S$; $\Delta C_{Rn}$ (Bq $m^{-3}$) is the added radon concentration within the build-up time of $\Delta T$ (min); $k_1$ and $k_2$ is the slopes of the fitted lines as shown in Figure 5, Bq $m^{-3}$ $min^{-1}$.

According to one-dimensional calculating model for steady-state surface radon exhalation rate indicated in the references [25,26], radon diffusion coefficient ($D$, $m^2$ $s^{-1}$) can be obtained by Eq. (10):

$$\frac{J_1}{J_2} = \frac{\tanh(h/L)}{\tanh(h/2L)} = \frac{2k_1}{k_2} \tag{10}$$

where $h$ is the height of the specimen, namely 25 mm or 100 mm; $L$ (m) is the radon diffusion length defined as $L=(D/\lambda)^{1/2}$.

(4) Determination of radon emanation fraction $f$

The radon emanation fraction was determined based on the former tests of radium content and radon exhalation rate. This parameter can be expressed as [27]:

$$f = \frac{J_1 S}{C_{Ra} M_{dry} \lambda} \tag{11}$$

where $M_{dry}$ (kg) is the dry mass of specimen as mentioned in the previous section.

## 3. Results and discussion

### *3.1. Physical properties of the rocklike material*

The statistical physical parameters of the rocklike material including dry density ($\rho_{dry}$), grain density ($\rho_{grain}$) and porosity ($\eta$) are presented in Table 3. The dry density and grain density of the rock-material vary in the ranges of 2.332–2.453 g $cm^{-3}$ and 2.505–2.673 g $cm^{-3}$, respectively. Apparently the relationships among these densities are $\rho_{dry} < \rho_{grain}$. The porosity calculated by using Eq. (3) varies in the ranges of 5.651–8.223%.

**Table 3.** Statistical physical parameters of the rocklike material.

| | Density | | Porosity |
|---|---|---|---|
| Parameters | $\rho_{dry}$ (g $cm^{-3}$) | $\rho_{grain}$ (g $cm^{-3}$) | $\eta$ (%) |
| Minimum | 2.332 | 2.505 | 5.651 |
| Maximum | 2.453 | 2.673 | 8.223 |
| Mean | 2.376 | 2.553 | 6.904 |
| Median | 2.372 | 2.541 | 6.752 |
| Std. dev. | 0.031 | 0.047 | 0.871 |

### *3.2. Mechanical properties of the rocklike material*

The statistical mechanical parameters of the rocklike material including elastic modulus ($E$), Poisson ratio ($\mu$), uniaxial compressive strength ($\sigma_c$), tensile strength ($\sigma_t$), cohesion ($c$) and internal friction angle ($\varphi$) are presented in Table 4. The elastic modulus and Poisson ratio of the rocklike material vary in the ranges of $2.219\times10^4$–$2.381\times10^4$ MPa and 0.229–0.272, respectively. The uniaxial compressive strength and tensile strength vary in the ranges of 59.850–73.160 MPa and 3.670–4.130 MPa, respectively. In relation to cohesion and internal friction angle, the values of the two parameters are 15.837 MPa and 55.979 °, respectively. The ratio of compressive strength to tensile strength reaches 17.6. That is to say, the compressive property of the rocklike material is much better than its tensile property, this is actually one of the most essential characteristic of rock [28].

### *3.3. Radioactive properties of the rocklike material*

The statistical radioactive parameters of the rocklike material including dose equivalent rate ($\dot{H}$), radium content ($C_{Ra}$), radon exhalation rate ($J$), radon emanation fraction ($f$), radon diffusion coefficient ($D$) and radon diffusion length ($L$) are presented in Table 5. The dose equivalent rates on the average are less than 0.4 μSv $h^{-1}$. The radium content, radon exhalation rate and emanation

fraction change within the ranges of $1.828\times10^{3}$–$2.146\times10^{3}$ Bq kg$^{-1}$, 0.013–0.065 Bq m$^{-2}$ s$^{-1}$ and 6.521–10.760%, respectively. With respect to the radon diffusive parameters (namely radon diffusion coefficient and radon diffusion length), they vary in the ranges of $0.006\times10^{-6}$–$0.051\times10^{-6}$ m$^2$ s$^{-1}$ and 6.521–10.760%, respectively. It must be referred that radon diffusion coefficient and radon diffusion length in the rocklike material are within the ranges ($D$=$0.009\times10^{-6}$–$0.032\times10^{-6}$ m$^2$ s$^{-1}$, $L$=0.068–0.124 m) given by Daoud and Renken [29], and slightly out of the ranges ($D$=$0.04\times10^{-6}$–$0.15\times10^{-6}$ m$^2$ s$^{-1}$, $L$=0.144–0.256 m) given by Renken and Rosenberg [30]. Hence it is confirmed that the method for determining radon diffusive parameters was of validity. Nevertheless, the standard deviations of the parameters like radon exhalation rate, emanation fraction diffusion coefficient and diffusion length are relatively much larger than the others as shown in Table 5, and these remarkable differences are to a great extent due to less numbers and different sizes of samples.

**Table 4.** Statistical mechanical parameters of the rocklike material.

| Parameters | $10^{-4}E$ (MPa) | $\mu$ | $\sigma_c$ (MPa) | $\sigma_t$ (MPa) | $c^a$ (MPa) | $\varphi^a$ (°) |
|---|---|---|---|---|---|---|
| Minimum | 2.219 | 0.229 | 59.850 | 3.670 | – | – |
| Maximum | 2.381 | 0.272 | 73.160 | 4.130 | – | – |
| Mean | 2.293 | 0.242 | 67.853 | 3.853 | 15.837 | 55.979 |
| Median | 2.283 | 0.237 | 68.515 | 3.790 | – | – |
| Std. dev. | 0.060 | 0.015 | 5.331 | 0.195 | – | – |

[a] According to Eq. (6) and the fitted equation shown in Figure 2, cohesion and internal friction angle of the rocklike material can be determined, they are in fact the calculated values. For convenience sake, they are here displayed on the "mean" columns.

**Table 5.** Statistical radioactive parameters of the rocklike material.

| Parameters | Dose equivalent rate | | $10^{-3}C_{Ra}$ (Bq kg$^{-1}$) | $J$ (Bq m$^{-2}$ s$^{-1}$) | $f$ (%) | $10^{6}D$ (m$^2$ s$^{-1}$) | $L$ (m) |
|---|---|---|---|---|---|---|---|
| | $\dot{H}_{25}$ (μSv h$^{-1}$) | $\dot{H}_{100}$ (μSv h$^{-1}$) | | | | | |
| Minimum | 0.230 | 0.320 | 1.828 | 0.013 | 6.521 | 0.006 | 0.054 |
| Maximum | 0.450 | 0.500 | 2.146 | 0.065 | 10.760 | 0.051 | 0.156 |
| Mean | 0.331 | 0.388 | 1.993 | 0.035 | 8.667 | 0.029 | 0.105 |
| Median | 0.320 | 0.370 | 1.991 | 0.031 | 8.693 | 0.029 | 0.105 |
| Std. dev. | 0.073 | 0.058 | 0.140 | 0.022 | 2.143 | 0.032 | 0.072 |

### *3.4. Comparisons of the rocklike material with prototype material*

For convenience of comparative analysis, the average parameter values (see Tables 3–5) were accordingly supposed to represent the true properties of the rocklike material. The granite samples taken from a stone factory in southern China served as the prototype material. The same methods as mentioned above were used to determine the properties of the granite sample. The physico-mechanical parameter ratios (also known as similarity ratio, denoted as $R_{\rho,\mathrm{dry}}$, $R_{\rho,\mathrm{grain}}$, $R_\eta$, $R_E$, $R_\mu$, $R_{\sigma,c}$, $R_{\sigma,t}$, $R_c$ and $R_\varphi$) and radioactive parameter ratio (denoted as $R_{\dot{H},25}$, $R_{\dot{H},100}$, $R_{C,\mathrm{Ra}}$, $R_J$, $R_D$, $R_L$, and $R_f$) of the granite sample to the rocklike material were shown in Figures 6 and 7, respectively.

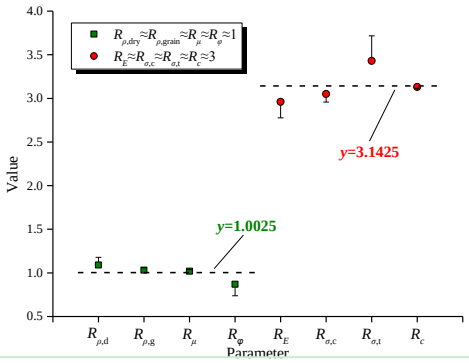


**Figure 6.** Similarity ratios about physico-mechanical parameters between prototype

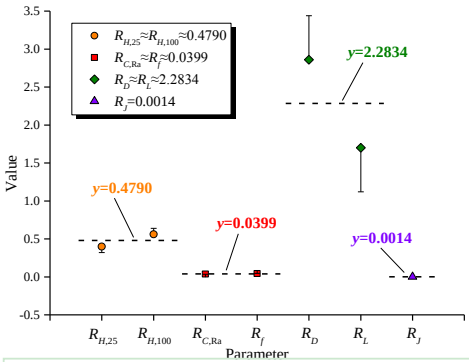


**Figure 7.** Similarity ratios about radioactive parameters between prototype material and

From Figure 6, it can be concluded that the relationships among these similarity ratios satisfy well to similarity theory [31]. However, similarity ratio of porosity has not been exhibited in Figure 6, since we found that the porosity of the rocklike material is five times as large as the granite sample's. Probably the distinct deviation is attributed to the relatively less proportion of silica fume. Besides, uranium ore-rock is of severe radioactivity, and most uranium deposits in China are granite-types. Therefore, we give up field sampling of uranium ore-rock as the prototype material, and turn to granite sample taken from a stone factory in southern China. Actually, the differences between the in-situ uranium ore-rock sample and granite sample are distinct, for example, hydroscopicity and seepage property of the former are much better than the latter. In this study, water absorption method has been utilized to estimate the sample's porosity, so the measured porosity is surely larger than the its real porosity.

Figure 7 indicates that radium content and radon emanation fraction of the rocklike material are much larger than those of the granite sample, exceeding 26 times and 22 times or so, respectively. These are the main causes that lead to a quite lower radon exhalation rate of the granite sample. However, both of the dose equivalent rates of the granite sample are close to half of those of the rocklike material, the sizes of the studied specimens are not large enough and that may account for the slight differences on dose equivalent rate. Moreover, though the radon diffusive parameters, including radon diffusion coefficient ($D$), radon diffusion length ($L$), have 0.5–2 times the gap between the two materials, they are still falling within the same order of magnitude. Specially, the values of remaining radioactive properties of the prepared material, like radon exhalation rate ($J$) and radium content ($C_{Ra}$) are within the same order of magnitude compared with Indian low-grade uranium ore reported by Sahu et al [27]. As to radon emanation fraction ($f$), Indian uranium ore is reported as 0.4–8.9 [27], the rhyolite and granite uranium ore from N. E. Nigeria are 0.22 and 0.31 respectively [6], and Australian uranium rock varies in the range of 0.1–0.3 [32]. The variations of emanation fraction may be attributed to some reasons, such as the differences of grain size, spatial distribution of radium, properties of porous network, water content and temperature in the materials. Therefore, radon emanation fraction of the prepared material can be considered reasonable.

## 4. Conclusions

This article reports how to prepare a novel radioactive rocklike material for radon research. Comparisons of the rocklike material with the prototype material (taken from a stone factory in South China) have been discussed. The results indicate that the prepared rocklike material possesses a favorable brittleness, this accords with a real rock material. On the whole, similarity ratios of physical and mechanical properties agree well with similarity theory. The values of radioactive properties of the prepared material are in general much larger than those of the granite sample; however, with respect to diffusive parameters (to some degree they can be regarded as physical properties), the situation reverses but they are still falling within the same order of magnitude. Actually, this proves our prepared radioactive rocklike material can be a reliable alternative for real radium-containing rock.

Moreover, through tuning the ratio of pure quartz sands and uranium mill tailings under the condition that their totals remain constant, we can obtain the rocklike materials with different levels of radioactivity. Similarly, those rocklike materials meeting different experimental requirements can also be fabricated using the proposed methods.

**Acknowledgement**

This work was supported by National Natural Science Foundation of China (NSFC) under funded project №11475081 and State Administration of Work Safety (SAWS) under funded project hunan-0022-2015AQ, we wish to express thanks to NSFC and SAWS.

**References**

[1] Laborde-Castérot H, Laurier D, Caër-Lorho S, Etard C, Acker A and Rage E 2014 *Occup. Environ. Med.* **71** 611–618
[2] George A C 2008 Nat. *Radiat. Environ.* **1034** 20–33
[3] Carrera G, Garavaglia M, Magnoni S, Valli G and Vecchi R 1997 *J. Environ. Radioactiv.* **34** 149–159
[4] Rafique M and Rathore M H 2013 *Int. J. Environ. Sci. Te.* **10** 1083–1090
[5] Arabi A S, Futua I I, Dewu B B M, Kwaya M Y, Kurowska E, Muhammad A M and Garba M L 2016 *Environ. Earth Sci.* **75** 1–9
[6] Funtua I I, Onojah A, Jonah S A, Jimba B W and Umar I M 1997 *Appl. Radiat. Isotopes* **48** 867–869
[7] Singh A K, Sengupta D and Prasad R 1999 *Appl. Radiat. Isotopes* **51** 107–113
[8] Kumar R, Sengupta D and Prasad R 2003 Radiat. *Meas.* **36** 551–553
[9] Mahur A K, Kumar R, Sonkawade R G, Sengupta D and Prasad R 2008 *Nucl. Instrum. Meth. B* **266** 1591–1597
[10] Holaday D A 1967 Radiol. *Heal. Data. Rep.* **8** 135–138
[11] Guo Y H, Cao R J and Zhu L H 2012 *Adv. Mater. Res.* **616-618** 346-349
[12] Shen Y J, Rong T L, Yang G S, Yuan Y Z, Yang Y and Yu X 2016 *Adv. Sci. Te. Water Resour.* **36** 75–79
[13] Sterpi D and Cividini A 2004 *Rock Mech. Rock Eng.* **37** 277–298
[14] Meguid M A and Mattar J 2009 *J. Geotech. Geoenviron.* **135** 973–979
[15] Zhu W S, Zhang Q B, Zhu H H, Li Y, Yin J H, Li S C, Sun L F and Zhang L 2010 *Can. Geotech. J.* **47** 935–946
[16] Heiskanen J 1992 *Commun. Soil Sci. Plan.* **23** 841-846
[17] Manger G E 1963 *Geol. Surv. Bull.* 1144-E
[18] Jaeger J C and Hoskins E R 1966 *J. Geophys. Res.* **71** 2651–2659
[19] Claesson J and Bohloli B 2002 *Int. J. Rock Mech. Min.* **39** 991–1004
[20] Andreev G E 1991 Min. *Sci. Te.* **13** 445–456
[21] Hank R J, Mccarty L E and Barber E S 1949 *Highway Research Board Proceedings* **28** 449–456
[22] Perrier F and Girault F 2012 *J. Environ. Radioactiv.* **113** 45–56
[23] Stoulos S, Manolopoulou M and Papastefanou C 2003 *J. Environ. Radioact.* **69** 225–240
[24] Sahoo B K, Nathwani D, Eappen K P, Ramachandran T V, Gaware J J and Mayya Y S 2007 *Radiat. Meas.* **42** 1422–1425
[25] Lei X, Zhang L and Guo Q J 2011 *Radiat. Prot.* **31** 13–16, 22
[26] Zhang L, Lei X, Guo Q J, Wang S Q, Ma X H and Shi Z L 2012 *J. Radiol. Prot.* **32** 315–323
[27] Sahu P, Mishra D P, Panigrahi D C, Jha V and Patnaik R L 2013 *J. Environ. Radioact.* **126** 104–114
[28] Gong Q M and Zhao J 2007 *Tunn. Undergr. Sp. Te.* **22** 317–324
[29] Daoud W Z and Renken K J 2001 *Sci. Total Environ.* **272** 127–135
[30] Renken K J and Rosenberg T 1995 *Health Phys.* **68** 800–808
[31] Xiao T L, Li X P and Jia S P 2012 Chinese *J. Rock Mech. Eng.* **31** 1666–1673
[32] Mudd G M 2008 *J. Environ. Radioact.* **99** 288–315